Article

Coassembly of Amphiphiles with Opposite Peptide Polarities into Nanofibers

Heather A. Behanna, Jack J. J. M. Donners, Alex C. Gordon, and Samuel I. Stupp

J. Am. Chem. Soc., **2005**, 127 (4), 1193-1200• DOI: 10.1021/ja044863u • Publication Date (Web): 07 January 2005

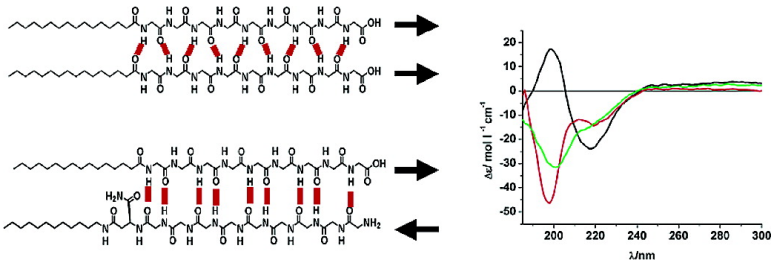

More About This Article

Additional resources and features associated with this article are available within the HTML version:

- Supporting Information
- Links to the 27 articles that cite this article, as of the time of this article download
- Access to high resolution figures
- Links to articles and content related to this article
- Copyright permission to reproduce figures and/or text from this article

View the Full Text HTML

J|A|C|S
ARTICLES
Published on Web 01/07/2005

Coassembly of Amphiphiles with Opposite Peptide Polarities into Nanofibers

Heather A. Behanna,[†] Jack J. J. M. Donners,[‡] Alex C. Gordon,[§] and Samuel I. Stupp*[,†,‡,§,||]

Contribution from the Department of Chemistry, Institute for BioNanotechnology in Medicine, Department of Materials Science & Engineering, and Feinberg School of Medicine, Northwestern University, Evanston, Illinois 60208

Received August 25, 2004; E-mail: s-stupp@northwestern.edu

Abstract: The design, synthesis, and characterization of "reverse" peptide amphiphiles (PAs) with free N-termini is described. Use of an unnatural amino acid modified with a fatty acid tail allows for the synthesis of this new class of PA molecules. The mixing of these molecules with complementary ones containing a free C-terminus results in coassembled structures, as demonstrated by circular dichroism and NOE/NMR spectroscopy. These assemblies show unusual thermal stability when compared to assemblies composed of only one type of PA molecule. This class of reverse PAs has made it possible to create biologically significant assemblies with free N-terminal peptide sequences, which were previously inaccessible, including those derived from phage display methodologies.

Introduction

Materials designed molecularly for regeneration of tissues are becoming of great interest in advanced medicine.[1−4] Scaffolds of synthetic polymers, including polymers based on L-lactic or glycolic acid,[5] and biopolymers, including collagen,[6] fibrin,[7] or alginate,[8] have been studied. One role of these scaffolds is to provide structural support to cells naturally provided by extracellular matrixes (ECM).[1] The synthetic scaffolds are more mechanically sound, but traditionally do not contain the cell signals found in ECM. More recently, both natural and synthetic scaffolds have been modified to contain peptides found in extracellular proteins that promote receptor-based interactions with cells[3,9−16] and have been used to promote cell adhesion or differentiation.[17−20]

Advances in self-assembly offer new opportunities in molecular design of biomaterials. Amphiphilic molecular building blocks can be assembled in aqueous environments to form scaffolds with well-defined and diverse chemical structures. Various classes of peptide-based amphiphiles have been reported in the literature, including amphiphilic peptides and peptides functionalized with alkyl tails on one or both termini. Amphiphilic peptides have been shown to form a variety of supramolecular-structure-like nanotapes,[21−23] ribbons,[23−25] fibers,[2,26−28]and twisted ribbons.[29,30] These structures originate from β-sheet formation between the self-assembling amphiphiles. A special case is the amphiphilic peptide block copolymers that form gels whose properties strongly depend on the secondary structure of the individual peptide blocks.[31]

[†] Department of Chemistry.
[‡] Institute for BioNanotechnology in Medicine.
[§] Department of Materials Science & Engineering.
[||] Feinberg School of Medicine.

(1) Lee, K.; Mooney, D. *Chem. Rev.* **2001**, *101*, 1869.
(2) Zhang, S. G. *Nat. Biotechnol.* **2003**, *21*, 1171.
(3) Hartgerink, J. D.; Beniash, E.; Stupp, S. I. *Proc. Natl. Acad. Sci. U.S.A.* **2002**, *99*, 5133.
(4) Hubbell, J. A. *Bio/Technology* **1995**, *13*, 565−576.
(5) Anderson, J. M.; Shive, M. S. *Adv. Drug Delivery Rev.* **1997**, *28*, 5.
(6) Kaufmann, P.; Heimrath, S.; Kim, B. S.; Mooney, D. J. *Cell Transplant* **1997**, *6*, 463.
(7) Schense, J. C.; Hubbell, J. A. *Bioconjugate Chem.* **1999**, *10*, 75.
(8) Draget, K. I.; SkjakBraek, G.; Smidsrod, O. *Int. J. Biol. Macromol.* **1997**, *21*, 47.
(9) Langer, R. *Acc. Chem. Res.* **2000**, *33*, 94.
(10) Vandermeulen, G. W. M.; Klok, H. A. *Macromol. Biosci.* **2004**, *4*, 383.
(11) Hirano, Y.; Mooney, D. J. *Adv. Mater.* **2004**, *16*, 17.
(12) Zhang, Y.; Gu, H. W.; Yang, Z. M.; Xu, B. *J. Am. Chem. Soc.* **2003**, *125*, 13680.
(13) Malkar, N. B.; Lauer-Fields, J. L.; Juska, D.; Fields, G. B. *Biomacromolecules* **2003**, *4*, 518.
(14) Boontheekul, T.; Mooney, D. J. *Curr. Opin. Biotechnol.* **2003**, *14*, 559.
(15) Santoso, S. S.; Vauthey, S.; Zhang, S. G. *Curr. Opin. Colloid Interface Sci.* **2002**, *7*, 262.
(16) Silva, G.; C, C.; Niece, K. L.; Beniash, E.; Harrington, D.; Kessler, J.; Stupp, S. I. *Science* **2004**, *303*, 1352.
(17) Holmes, T. C.; de Lacalle, S.; Su, X.; Liu, G. S.; Rich, A.; Zhang, S. G. *Proc. Natl. Acad. Sci. U.S.A.* **2000**, *97*, 6728.
(18) Borkenhagen, M.; Clemence, J.; Sigrist, H.; Aebischer, P. *J. Biomed. Mater. Res.* **1998**, *40*, 392.
(19) Sultzbaugh, K.; Speaker, T. *J. Microencapsulation* **1996**, *13*, 363.
(20) Rowley, J.; Madlambayan, G.; Mooney, D. *Biomaterials* **1999**, *20*, 45.
(21) Aggeli, A.; Bell, M.; Boden, N.; Keen, J. N.; McLeish, T. C. B.; Nyrkova, I.; Radford, S. E.; Semenov, A. *J. Mater. Chem.* **1997**, *7*, 1135.
(22) Aggeli, A.; Bell, M.; Boden, N.; Keen, J. N.; Knowles, P. F.; McLeish, T. C. B.; Pitkeathly, M.; Radford, S. E. *Nature* **1997**, *386*, 259.
(23) Aggeli, A.; Nyrkova, I. A.; Bell, M.; Harding, R.; Carrick, L.; McLeish, T. C. B.; Semenov, A. N.; Boden, N. *Proc. Natl. Acad. Sci. U.S.A.* **2001**, *98*, 11857.
(24) Aggeli, A.; Bell, M.; Carrick, L. M.; Fishwick, C. W. G.; Harding, R.; Mawer, P. J.; Radford, S. E.; Strong, A. E.; Boden, N. *J. Am. Chem. Soc.* **2003**, *125*, 9619.
(25) Matsumura, S.; Uemura, S.; Mihara, H. *Chem.—Eur. J.* **2004**, *10*, 2789.
(26) Altman, M.; Lee, P.; Rich, A.; Zhang, S. G. *Protein Sci.* **2000**, *9*, 1095.
(27) Goeden-Wood, N. L.; Keasling, J. D.; Muller, S. J. *Macromolecules* **2003**, *36*, 2932.
(28) Zhang, S.; Holmes, T. C.; Lockshin, C.; Rich, A. *Proc. Natl. Acad. Sci. U.S.A.* **1993**, *90*, 3334.
(29) Marini, D. M.; Hwang, W.; Lauffenburger, D. A.; Zhang, S. G.; Kamm, R. D. *Nano Lett.* **2002**, *2*, 295.
(30) Vauthey, S.; Santoso, S.; Gong, H. Y.; Watson, N.; Zhang, S. G. *Proc. Natl. Acad. Sci. U.S.A.* **2002**, *99*, 5355.
(31) Nowak, A. P.; Breedveld, V.; Pakstis, L.; Ozbas, B.; Pine, D. J.; Pochan, D.; Deming, T. J. *Nature* **2002**, *417*, 424.

An example of peptide amphiphiles with alkyl tails on one terminus includes amphiphiles derived from peptide motifs found in collagen, which result in the formation of triple helical units that form spheroidal or disklike micellar structures depending on the tail length and number of tails.[32−34] Another class has two tails, one per terminus. These amphiphiles display amyloid-like behavior in that they undergo a transition from a random coil to β-sheet-type hydrogen bonding upon increasing the concentration to form fibrillar structures.[35−39] There are reports of purely peptidic nanostructures with antiparallel arrangements,[21] and one report of two modified peptide amphiphiles that aggregate in an antiparallel arrangement driven by an unnatural alkylated quaternary ammonium salt.[39]

Our laboratory reported earlier on a class of peptide amphiphiles (PAs) that consist of a linear hydrophobic tail coupled to a peptide block that includes β-sheet-forming segments, charged residues for solubility, and biological epitopes.[3,40] The alkyl tail is attached to the N-terminus of the peptide, and the epitope segment is placed at the C-terminus. Upon application of a trigger such as a change in pH or ion concentration, these PA molecules self-assemble in aqueous solution into nanofibers.[3,40] The alkyl chains are in the core of the fibers, with the epitopes displayed on the periphery for cell interaction. Epitopes that have been incorporated into the PA molecules mimic extracellular matrix proteins and promote cell adhesion or differentiation through cell signaling.[16] It has also been shown that two different PA molecules with different epitopes and complementary charge can be coassembled into the same nanofiber.[41]

We report here on a new class of peptide amphiphiles that lead to structures in which the peptide sequence has reverse polarity. Solid-phase synthesis typically requires that peptide segments be synthesized from the C-terminus to the N-terminus. Therefore, previously reported PAs have been prepared by capping the free N-terminus by an alkyl tail, resulting in PAs with either a free acid or a free amide group presented on the periphery. In nature, bioactive sequences have different requirements for activity, including, in some cases, a free N-terminus.[42,43] A method to such peptides has been reported utilizing postmodification of lysine residues.[44−46] Since this method is incompatible with acid-labile resins, a new route was developed based on the introduction of the alkyl tail on an unnatural amino acid that can be coupled to the resin. We term the PAs from this method "reverse" PAs, and have investigated their synthesis via routine Fmoc solid-phase methodology.

Chart 1. Chemical Structures of Peptide Amphiphiles

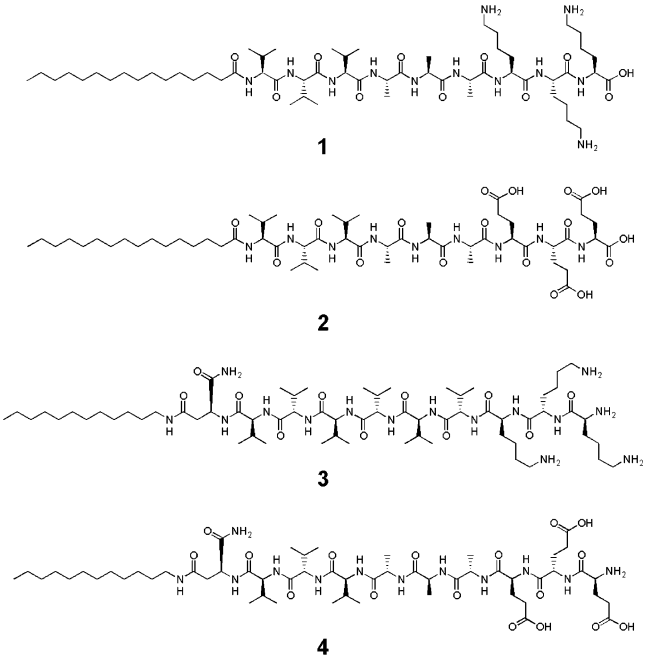

Having access to amphiphiles with both peptide polarities, we have also investigated here their coassembly. This has included coassembly of one PA with a phage-display-derived peptide sequence for bioactivity purposes.[47] The use of any phage-derived sequence in the coassembled structures is only possible as a result of our new synthetic strategy. We show below a schematic representation of the aggregation of peptide amphiphiles of identical and opposite polarities and their expected arrangements:

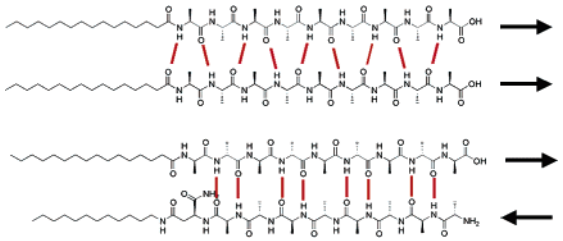

The secondary structure and thermal stability of the coassembled PAs is investigated by circular dichroism (CD), NMR, and FT-IR.

Results and Discussion

Four PAs, two with a triple lysine sequence (**1, 3**) and two with a triple glutamic acid sequence (**2, 4**), were prepared (Chart 1). PAs **1** and **2** were prepared by standard Fmoc solid-phase peptide techniques using a preloaded Wang resin followed by alkylation with palmitic acid with 2-(1*H*-benzotriazole-1-yl)-1,1,3,3-tetramethyluronium hexafluorophosphate (HBTU) as a coupling reagent. The amphiphile was cleaved from the resin with a mixture of 95% trifluoroacetic acid (TFA), 2.5% water, and 2.5% triisopropylsilane (TIS). For the synthesis of peptide amphiphiles **3** and **4**, amino acid **7** was synthesized according to Scheme 1. *N*-Carbobenzyloxy-L-aspartic anhydride was reacted with dodecylamine, yielding fatty acid amino acid **5**.

(32) Gore, T.; Dori, Y.; Talmon, Y.; Tirrell, M.; Bianco-Peled, H. *Langmuir* **2001**, *17*, 5352.
(33) Yu, Y. C.; Tirrell, M.; Fields, G. B. *J. Am. Chem. Soc.* **1998**, *120*, 9979.
(34) Yu, Y. C.; Berndt, P.; Tirrell, M.; Fields, G. B. *J. Am. Chem. Soc.* **1996**, *118*, 12515.
(35) Ganesh, S.; Jayakumar, R. *Biopolymers* **2003**, *70*, 336−345.
(36) Ganesh, S.; Prakash, S.; Jayakumar, R. *Biopolymers* **2003**, *70*, 346.
(37) Yamada, N.; Ariga, K.; Naito, M.; Matsubara, K.; Koyama, E. *J. Am. Chem. Soc.* **1998**, *120*, 12192.
(38) Yamada, N.; Komatsu, T.; Yoshinaga, H.; Yoshizawa, K.; Edo, S.; Kunitake, M. *Angew. Chem., Int. Ed.* **2003**, *42*, 5496.
(39) Yamada, N.; Ariga, K. *Synlett* **2000**, 575.
(40) Hartgerink, J. D.; Beniash, E.; Stupp, S. I. *Science* **2001**, *294*, 1684.
(41) Niece, K. L.; Hartgerink, J. D.; Donners, J.; Stupp, S. I. *J. Am. Chem. Soc.* **2003**, *125*, 7146.
(42) Biesecker, G.; Harris, J. I.; Thierry, J. C.; Walker, J. E.; Wonacott, A. J. *Nature* **1977**, *266*, 328.
(43) Sun, X. X.; Wang, C. C. *J. Biol. Chem.* **2000**, *275*, 22743.
(44) Gariepy, J.; Remy, S.; Zhang, X.; Ballinger James, R.; Bolewska-Pedyczak, E.; Rauth, M.; Bisland Stuart, K. *Bioconjugate Chem.* **2002**, *13*, 679.
(45) Geahlen, R. L.; Loudon, G. M.; Paige, L. A.; Lloyd, D. *Anal. Biochem.* **1992**, *202*, 68.
(46) Kruger, R. G.; Dostal, P.; McCafferty, D. G. *Chem. Commun.* **2002**, 2092.
(47) Smith, G. P. *Chem. Rev.* **1997**, *97*, 391.

Scheme 1. Synthesis of Fatty Acid Amino Acid **7**

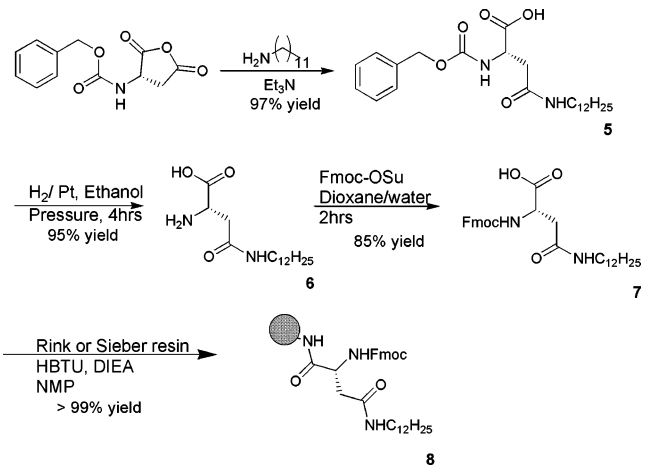

The CBz group was then removed by catalytic hydrogenation to yield **6**, followed by Fmoc protection of the amine. This synthesis proceeds readily on a 5 g scale. Product **7** was then coupled to a Rink resin using HBTU as a coupling reagent. Subsequently, the remaining amino acids were added to **8** using standard Fmoc solid-phase techniques. Standard cleavage conditions yielded PAs with reverse structure as previously described. ^{1}H NMR and electrospray ionization mass spectrometry are consistent with the expected structures.

When dispersed in aqueous media in the presence of suitable stimuli, PAs typically self-assemble into high aspect ratio cylindrical nanofibers.[3,40,41] On the basis of previous work, we expected that fibers consisting of either one PA molecule or a mix of two PA molecules would show secondary structures with β-sheet-like hydrogen bonding. It was anticipated that mixing of the negatively charged **2** or **4** with oppositely charged **1** or **3,** respectively, would result in parallel β-sheet-like hydrogen-bonding arrangements, while mixing **1** or **2** with amine-terminated oppositely charged **4** or **3**, respectively, could result in antiparallel arrangements.

At a concentration of 0.1 mM, the CD spectra of **2**−**4** revealed peptide segments with predominantly random coil character (Figure 1). This most likely results from electrostatic repulsion among the highly charged molecules. Upon a change of pH to neutralize the charges or upon addition of calcium ions, all PAs exhibited β-sheet signatures (Figure 1). In contrast, **1** exhibits a β-sheet signature under any pH. **1** may be less charged than the others, since the acid terminus can neutralize the charge of one of the lysine residues, giving the molecule a formal net charge of +2. This lower overall charge may reduce repulsion and allow β-sheet hydrogen bonding within the fibers to take place. Conversely, **4** would have a formal net charge of −2, as the amine terminus would neutralize the charge of one of the glutamic acid residues, allowing for the β-sheet interactions to occur. However, **4** still exhibited a disordered CD signature. To resolve this apparent contradiction, the actual charge state of and apparent pK_a of the aggregates at pH 7 were determined to better understand the driving forces for self-assembly of these various systems.

pH titrations of aggregates of molecules **1**−**4** were carried out at a concentration of 3 mM. All titrations were started at a pH where the molecules were already in their aggregated state to avoid kinetic effects due to self-assembly. Only the pK_a

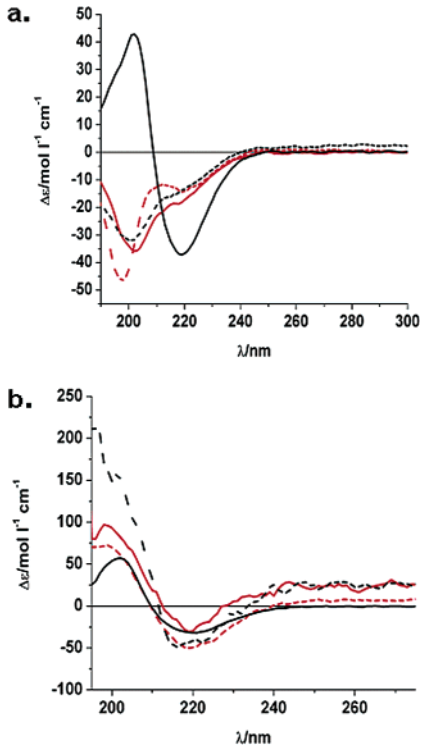

Figure 1. (a) CD spectra of **1** (black, solid), **2** (red, dashed), **3** (black, dashed), and **4** (red, solid). (b) Same series after the addition of acid (**2**, **4**) or base (**1**, **3**). Samples were diluted 4-fold due to increased ion concentration.

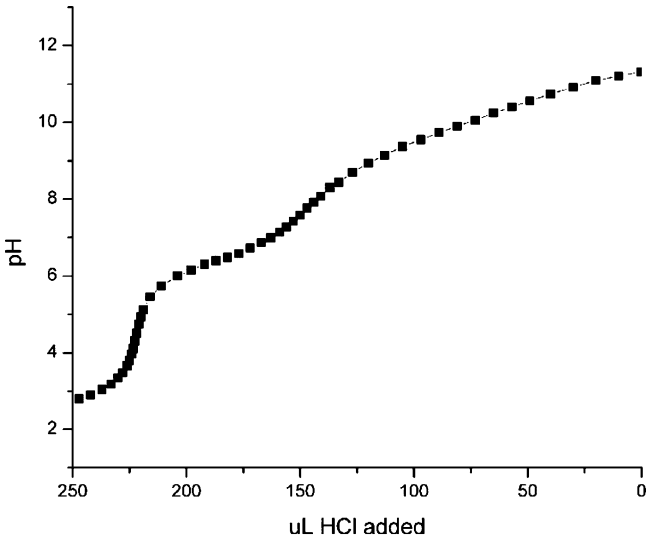

Figure 2. Titration of 0.1 N HCl to aggregates of PA **3** at a concentarion of 3 mM.

titration of **3** showed sharp transitions (Figure 2), correlating to two apparent pK_a values, one attributed to the deprotonation of the more solvent accessible amine terminus, and the other originating from one or more of the ϵ-lysine amines. As seen in the Supporting Information, aggregates of PAs **1**, **2**, and **4** show complex curves with transitions occurring over wide ranges, implying that the protonation/deprotonation of these supramolecular objects occurs slowly, with variations of acidity due to the local microenvironments within the nanofibers. It is clear from these results that aggregation changes the apparent pK_a values of the acid and amine groups, consistent with recent reports in the literature.[48]

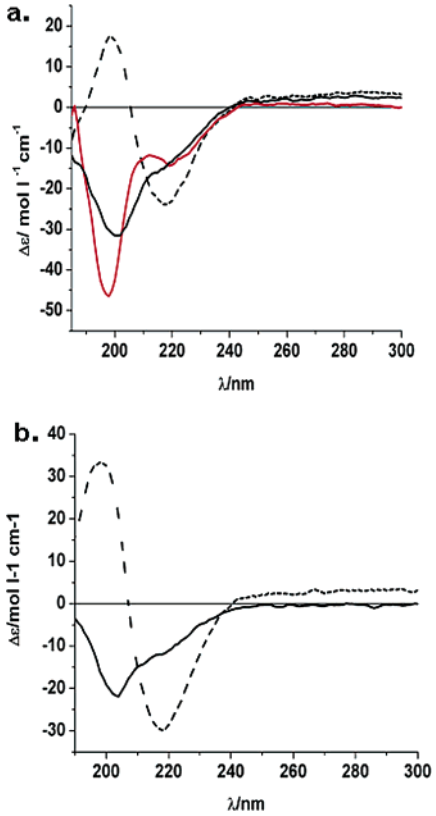

Figure 3. (a) Coassembly of charge-complementary PAs **2** (red) and **3** (black) in a 1:1 ratio (dashed). (b) Coassembly of glutamic acid PAs **2** and **4** (solid) and lysine PAs **1** and **3** (dashed).

We expect that coassembly of charge-complementary PA molecules should lead to fibers containing a mix of the two components with β-sheet hydrogen-bonding arrangements. When **2** is mixed with the triple lysine amphiphile **3** or **1** (abbreviated as **2/3** or **2/1)**, the CD spectrum obtained corresponds to a pure β-sheet (Figure 3). The fact that the observed β-sheet signature is not merely a superposition of individual CD spectra of the two components strongly suggests the formation of mixed nanofibers in which two molecules form a single aggregate structure. PA **1** mixed with the triple glutamic acid PA **4** or **2** (**1/4** or **1/2**) exhibits similar behavior (see the Supporting Information). When two PAs of similar charge are mixed, the **1/3** lysine mixture shows a β-sheet, whereas the **2/4** glutamic acid mixture shows a disordered conformation, possibly due to greater charge repulsion among the glutamic acid residues (Figure 3).

To further demonstrate coassembly of the molecules within the fibers, nuclear Overhauser effect (NOE) spectroscopy was performed on a 1.5 wt % gel made up of the charge-complementary PAs. A representative NOESY of **2** and **3** (**2/3)** is shown in Figure 6. Close contacts (<3 Å) were observed between the Glu-H_β protons of **2** and the Lys-H_ϵ and Val-H_δ protons of **3**, respectively (Figure 4). Several other possible intermolecular contacts were detected but could not be attributed unambiguously to **2/3** contacts. These results provide additional evidence that the two PA molecules are coassembled within the same nanofiber.

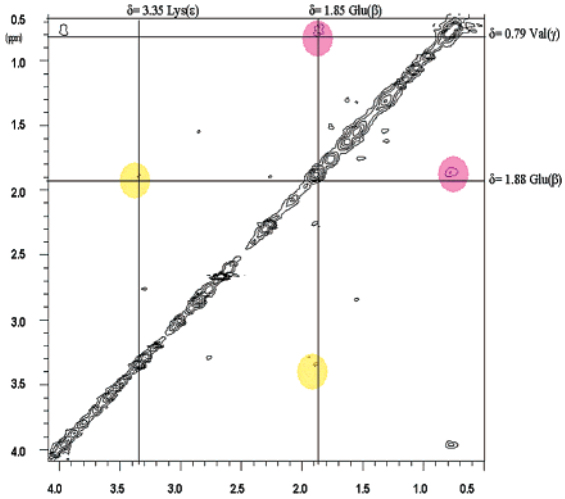

Figure 4. NOESY spectrum of **2/3**. Close contacts are indicated by the colored circles.

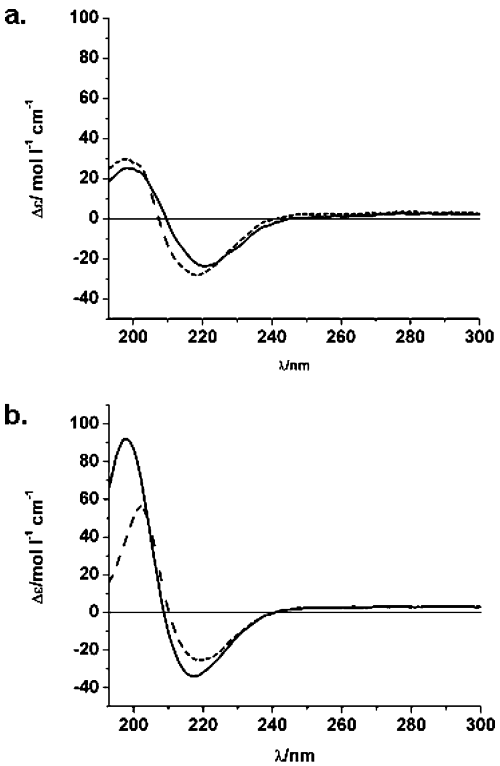

Figure 5. CD spectra of **2/3** (solid) and **1/2** (dashed) at (a) room temperature and (b) after heating for 2 h at 80 °C.

We used CD to investigate the potential parallel vs antiparallel alignment of the PA molecules in the assembled systems. Theoretical calculations have shown that antiparallel β-sheets have a maximum that is shifted to slightly lower wavelengths and a second crossover around 185 nm rather than at 190 nm for the parallel case.[49,50] The **2/3** mixture was expected to form an antiparallel arrangement as compared to the **1/3** pair, which is anticipated to have a parallel arrangement. However, no clear difference was observed between the two systems (Figure 5). No change in the CD signal was observed upon aging samples

(48) Ohaski, M.; Okuda, T.; Wada, A.; Hirayama, T.; Niidome, T.; Aoyagi, H. *Bioconjugate Chem.* **2002**, *13*, 510.
(49) Balcerski, J. S.; Pysh, E. S.; Bonora, G. M.; Toniolo, C. *J. Am. Chem. Soc.* **1976**, *98*, 3470.
(50) Kelly, M. M.; Pysh, E. S.; Bonora, G. M.; Toniolo, C. *J. Am. Chem. Soc.* **1977**, *99*, 3264.

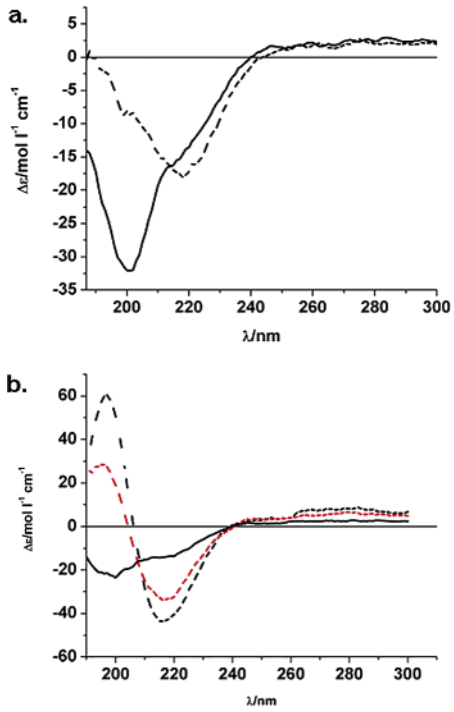

Figure 6. (a) VT-CD spectra of **3** at room temperature (solid) and 85 °C (dashed). (b) Dilution of **3** from 0.125 mg/mL (solid black) to 0.04 mg/mL (dashed black).

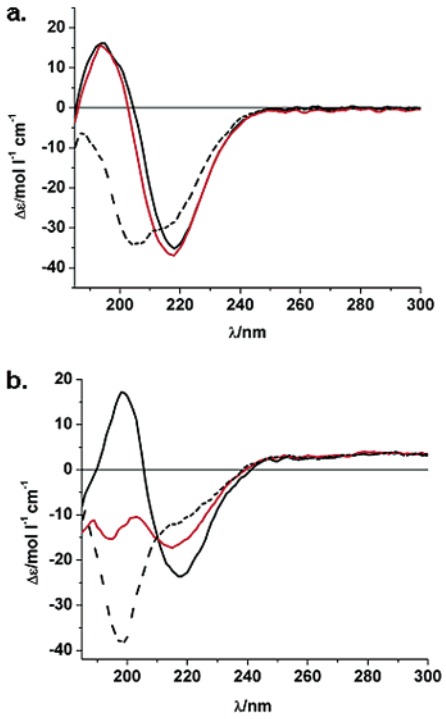

Figure 7. Increase of the ratio of the glutamic acid PAs **4** and **2** in the systems with opposite peptide polarity: (a) **4/1** and (b) **2/3**. Mixes were prepared in the ratios of 1:1 (black, solid), 2:1 (red, solid), and 10:1 (black, dashed).

at room temperature or after ultrasonication (see the Supporting Information). We therefore annealed the mixtures to facilitate self-assembly by heating the samples to 80 °C for 2 h, resulting in a significant increase in CD signal intensity (Figure 5). Prolonged annealing at 37 °C (24 h) produced results similar to those of annealing at 80 °C for **2/3**. For the **1/3** mixture, the benefit of annealing was less pronounced (see the Supporting Information). The annealing of the mixtures elucidated differences between the **1/2** and **2/3** coassembled nanofibers (Figure 5). In the **1/2** system, the peak maximum is at 202 nm compared to 197 nm for **2/3**, while at 190 nm, the Cotton effect of **1/2** appears to approach zero and for the **2/3** system a positive Cotton effect is still observed. Whereas these results could be indicative of an antiparallel arrangement for **2/3,** the present data do not allow the exclusion of mixed arrangements. However, it is evident that the coassembly of opposite-polarity PAs leads to a packing arrangement different from that from coassembly of PAs with identical polarity.[50] Furthermore, the spectra show an increase of peak intensity by a factor of 2 for **1/2**, whereas the **2/3** system shows an increase by a factor of 4 (Figure 5). This indicates that the **2/3** system has a longer coherence length arising from larger domains of coupled amide chromophores along the fiber axis, which in turn implies that the arrangement of hydrogen bonding that arises in the **2/3** system appears to be more energetically favorable than the **1/2** arrangement. Clearly, the initial coassembled structures are not at equilibrium but become more stable by annealing, either at 37 °C, which is physiologically relevant, or more rapidly at 80 °C.

A series of variable-temperature CD (VT-CD) experiments were carried out to study further the mechanism of self-assembly in mixed systems. Samples were ramped in 5 °C increments from room temperature to 85 °C, and allowed to equilibrate for 5 min at each temperature before the spectra were recorded. For both the **1/2** and **2/3** systems, a steady increase of peak intensity is observed as temperature increases, and this increase is irreversible. The end temperature is well above the expected melting temperatures for the hydrogen-bonding networks (ca. 40−45 °C) and the aliphatic tails (ca. 60 °C), demonstrating the extraordinary stability of these supramolecular systems. The stepwise annealing process showed differences in peak maxima and crossover points between the two systems similar to those seen for the previous annealed samples (see the Supporting Information). This gradual shift suggests that the molecules rearrange to form more perfect β-sheets within the fibers upon heating.

The irreversible increase in signal intensity observed for the mixed systems was in stark contrast to the increase in signal intensity observed for those systems containing a single PA molecule. Upon heating, the spectra for these nanofibers gradually transition from disordered to a more ordered signature resembling a random coil to β-sheet transition (Figure 6). Upon cooling, this trend is reversed. We believe that, in this case, the fibers disassemble into individual molecules at high temperatures and reassemble upon cooling. This implies that the signature at elevated temperatures originates from individual PA molecules, and to confirm this, dilution studies were performed. At a concentration of approximately 0.7 mM, the random coil signature is replaced by a signature that more resembles a β-sheet (Figure 6), implying that this is the critical micelle concentration. The nonlinear decrease of the intensity confirms that the signature arises from a disassembled state.

Another probe into the nature of mixing was to change the ratios of the individual PAs in the pairs with opposite peptide polarities. A series of **1/4** and **2/3** mixtures were studied before and after annealing overnight at 37 °C. For both mixtures, an excess of the glutamic acid PA **4** or **2** led to a decrease of β-sheet

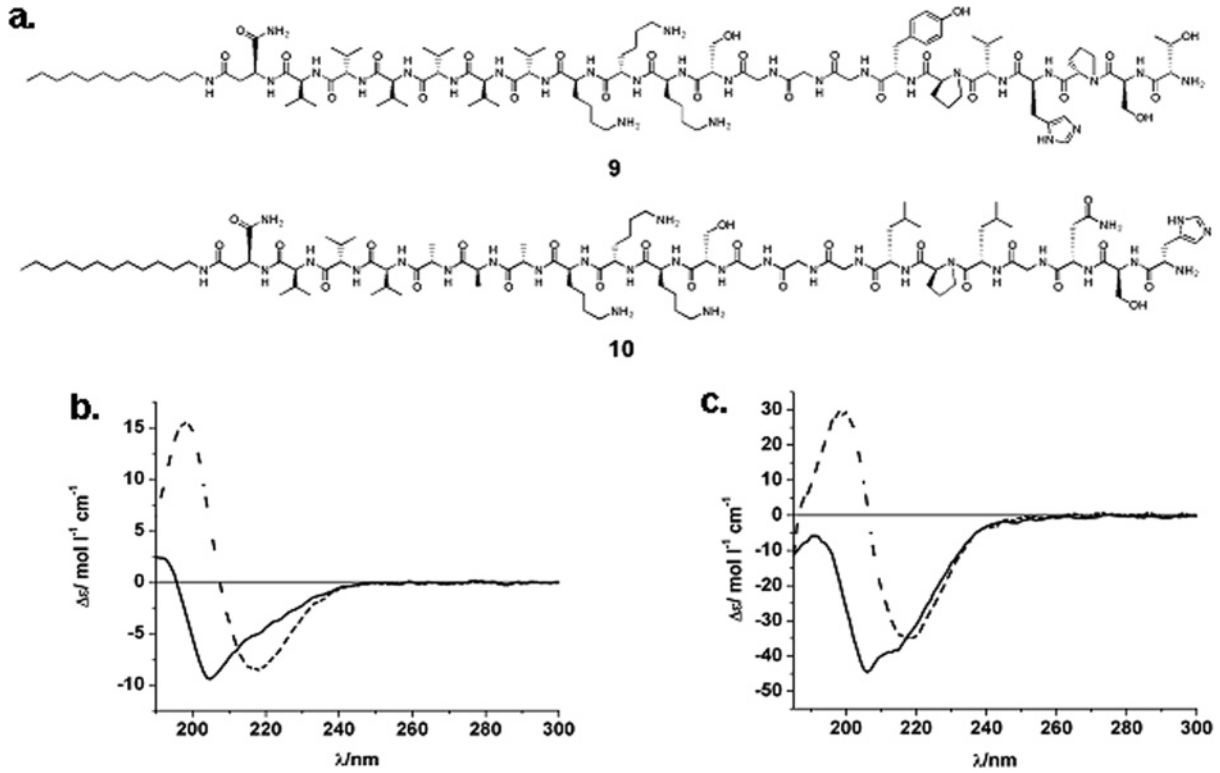

Figure 8. (a) Structures of BMP-2 binding PA **5** and TGF-β1 binding PA **6**. (b) CD spectra of **6** (solid) and **2/6** mixed 1:1 (dashed). (c) CD spectra of **3/5** mixed 49:1 and **2/3/5** mixed 50:49:1.

character, especially for **2** (Figure 7). In contrast, when a 2−10-fold excess of the lysine PA **1** or **3** was added, the β-sheet signature persisted for longer, and for **1** the β-sheet never diminishes (see the Supporting Information). The annealed series of mixtures show the same pattern (data not shown). It is apparent that the systems can tolerate a larger amount of **1** and **3**. These PAs both have the triple lysine sequence, but one of them has a free amine terminus and one a free acid terminus (Chart 1). It appears that charge is an important factor determining the secondary structure, as **1** and **3** are presumably less highly charged. It is known that lysine itself has a very broad pK_a transition and is only partially charged at physiological pH.[48]

IR spectroscopy was also performed on nanofibers composed of individual PAs as well as on the coassembled systems. To obtain the best signal-to-noise ratio, attenuated concentrations were 2 orders of magnitude higher than in the CD experiments and twice as high as gelation conditions. The PAs were dissolved in water at 2 wt % and then lyophilized. All the spectra exhibit the amide I frequency of 1627 cm^{-1} typical of β-sheets (see the Supporting Information). Many of the spectra display broad shoulders on this main peak, ranging from 1655 to 1700 cm^{-1}. These shoulders are indicative of other secondary structures such as antiparallel alignment of the hydrogen bonds. However, recent work by Surewicz et al. shows that the positions of these peaks are unreliable indicators to assign the secondary structures.[51] Therefore, we believe that the CD results are more reliable for investigating the packing arrangements of the peptide segments.

Once the successful coassembly of the amphiphiles was established, the gelation behavior of the systems from both single and multiple PAs was investigated. One weight percent solutions of **1**−**4** were slightly opaque and could be gelled by the addition of acid (**1**, **3**) or base (**2**, **4**). Transmission electron microscopy reveals the formation of nanofibers with average diameters of 6.5 nm and average lengths of several hundred nanometers, similar to those observed previously in other PAs (data not shown).[3]

As pointed out before, the systems studied in this work may be designed for biological activity. Our laboratory has recently identified two peptide binding sequences via phage display that bind growth factors bone morphogenetic protein-2 (BMP-2) and transforming growth factor β_1 (TGF-β), important in stem cell differentiation. These sequences each require a free N-terminus, and we were therefore able to use our new methodology to create PAs with these sequences. Each sequence was incorporated into a reverse PA as an extension of **3** on the N-terminal side to create PA molecules designed to bind BMP-2 (**9**) and TGF-β1 (**10**) (Figure 8). Of interest are the potentially bioactive coassemblies of these PAs with a PA such as **2** that has complementary charge and opposite peptide polarity. This will allow for presentation of the binding sequences on the periphery of the fibers. Both the **2/5** and **2/6** systems behave similarly to the model system **2/3** described before (Figure 8). For their use in biological applications, it is desirable to be able to form stable coassemblies with **5** and **6** significantly diluted in the nanofiber. However, this dilution was shown in the model systems to disrupt β-sheet character. The problem was solved by the use of the lysine PA **3** as an additional component. CD spectroscopy shows that a ternary mixture of **2**, **3**, and **5** (50:49:1) maintains β-sheet character (Figure 8), demonstrating that in this way dilution of growth factor binding sequences is possible while structural integrity is maintained.

(51) Surewicz, W. K.; Mantsch, H. H.; Chapman, D. *Biochemistry* **1993**, *32*, 389.

Conclusion

We have developed a synthetic strategy for peptide amphiphile molecules with free N-termini compatible with standard solid-phase methodology. When mixed with free C-terminus PAs, these molecules self-assemble into nanofibers containing highly thermally stable β-sheet structures which appear to be more stable than coassemblies of PAs with identical polarity. The new opportunity to create assemblies with free N-termini on their surfaces enables the design of bioactive nanofibers not accessible previously with nanostructures that expose the C-terminus of the peptide sequence.

Experimental Methods

General Information. All resins and Fmoc-L-amino acids were obtained from Novabiochem (San Diego, CA). All reagents for solid-phase synthesis were of synthesis grade and obtained from Applied Biosystems (Foster City, CA). All other reagents were obtained from Aldrich Chemical Co. (Milwaukee, WI) and were used as received. Solvents for solid-phase peptide synthesis were acquired from Applied Biosystems and were peptide synthesis grade. Other solvents were obtained from Fisher Scientific and were used as received unless stated otherwise.

PAs were synthesized using an Applied Biosystems 433A automated peptide synthesizer. NMR spectra were acquired on a Varian Inova 500 MHz spectrometer at room temperature. Electrospray mass spectra were collected on a Micromass Quattro II triple quadrupole HPLC/MS/MS mass spectrometer. CD spectra were recorded on a Jasco J-715 spectropolarimeter with a Jasco PTC-348WI Peltier-effect temperature controller. FT-IR spectra were run on a BioRad FTS-40 FT-IR machine, from 400 to 4000 nm with a 2 cm^{-1} resolution.

***N*-Dodecyl-2-carbobenzyloxyaminosuccinamic Acid (5).** *N*-Carbobenzyloxy-L-aspartic anhydride (1 mmol) was dissolved in 50 mL of methylene chloride, followed by the addition of 1.05 equiv of dodecylamine and 1.1 equiv of triethylamine. The reaction was capped to prevent evaporation, and stirred for 12 h. When no trace of starting material could be detected by thin-layer chromatography (TLC) (CH_2Cl_2, 5% MeOH), the reaction was quenched with 20 mL of 1 N hydrochloric acid followed by extraction with chloroform (5×). The organic layer was dried over magnesium sulfate, and **5** was obtained as a white solid (yield 97%). ^{1}H NMR ($CDCl_3$): δ 0.8 (t, J = 8.5 Hz, 3H, tail CH_3), 1.18 (s, 18H C_9H_{18} tail), 1.48 (br s, 2H, CONH*CH*$_2$), 2.68 (s, 2H,CONHCH$_2$*CH*$_2$), 3.15 (br s, 2H, Asp H$_\beta$), 4.49 (m, 1H, Asp H$_\alpha$), 5.12 (s, 2H, Ph*CH*$_2$O), 7.28 (s, 5H, Ph). ^{13}C (DMSO-d_6) δ 14.6, 22.8, 29.4, 29.6, 29.7, 32.0, 52.2, 56.7, 66.1, 128.4, 129.0, 137.7, 156.5, 171.1, 172.5. ESI MS: m/z 435.4 (MH^+).

2-Amino-*N*-dodecylsuccinamic Acid (6). In 100 mL of ethanol, 100 mmol of **5** was dissolved and transferred to a reaction vessel containing Pd and C (10 wt %). The vessel was then placed under hydrogen (35 Torr) for 3 h. The reaction mixture was filtered over Celite, and the product obtained as a white solid after evaporation to dryness under reduced pressure (yield 95%). ^{1}H NMR (CD_3CN): δ 1.15 (m, 23H, aliphatic tail), 1.3 (m, 2H, CONH$_2$CH$_2$*CH*$_2$), 2.37 (br s, 2H, CONH$_2$*CH*$_2$), 3.55 (m, 3H, Asp H$_\beta$), 4.6 (m, 1H, Asp H$_\alpha$). ESI MS: m/z 301.2 (MH^+).

***N*-Dodecyl-2-Fmoc-aminosuccinamic Acid (7).** In 200 mL of a water/dioxane (1:1 v/v) mixture, 6.6 mmol of **6** was dissolved with 1.3 mL (1.5 equiv) of triethylamine followed by 1 equiv of Fmoc-*O*-succinimide (Fmoc-OSu). The reaction was monitored by TLC (CH_2Cl_2, 10% MeOH), and after 2−3 h, all of the Fmoc-OSu was consumed. The reaction was quenched with acid, resulting in a white precipitate that was collected by filtration (yield 85%). ^{1}H NMR (DMSO-d_6): δ 0.84 (t, J = 8 Hz, 3H, terminal aliphatic CH_3), 1.19 (s, 18H, aliphatic CH_2), 1.34 (s, 2H, NH$_2$CH$_2$*CH*$_2$), 2.61 (br s, 2H, CONH*CH*$_2$), 3.08 (s, 2H, Asp H$_\beta$), 4.24 (m, 3H, Asp H$_\alpha$ + Fmoc-*CH*$_2$CONH + Fmoc-*CH*), 7.3 (t, J = 9 Hz, 1H, Fmoc-H), 7.39 (t, J = 9 Hz, 1H, Fmoc-H), 7.68 (d, J = 8.5 Hz, 1H, Fmoc-H), 7.85 (d, J = 9 Hz, 1H, Fmoc-H). ^{13}C (DMSO-d_6): δ 14.6, 22.8, 29.4, 29.5, 29.7, 32.0, 46.1, 47.3, 52.2, 6.7, 120.8, 126.0, 127.7, 128.3, 141.5, 144.5, 156.5, 171.1, 172.5. ESI MS: m/z 524 (MH^+).

PA Synthesis and Purification. PAs **1** and **2** were prepared as described in ref 3. For PAs **3**−**6**, the standard Rink resin was placed in a reaction vessel, deprotected three times with 30% piperidine in NMP, and then coupled to 2 equiv of **7** overnight. Coupling was repeated until a ninhyndrin test showed negative results. This modified resin **8** was then loaded onto the automated synthesizer, and peptide synthesis proceeded as for PAs **1** and **2**. When the automated synthesis was complete, the PA was cleaved from the resin as described in ref 3.

Data for $C_{15}H_{31}$CONH-Val-Val-Val-Ala-Ala-Ala-Lys-Lys-Lys-COOH (1). ^{1}H NMR (DMSO-d_6): δ 0.80−0.84 (m, 21H, Val$_\gamma$ + tail CH_3), 1.22 (br s, 28H, C_{14} aliphatic tail), 1.36 (m, 6H, Ala H$_\beta$), 1.51 (m, 11H, Lys H$_\gamma$ + tail *CH*$_2$CH$_2$CONH), 1.62 (m, 6H, Lys H$_\beta$), 1.91 (m, 9H, Val H$_\beta$ + Lys H$_\delta$), 2.16 (m, 2H, tail *CH*$_2$CONH), 2.73 (s, 6H, Lys H$_\epsilon$), 4.10−4.23 (m, 9H, H$_\alpha$), 7.6−8.1 (amide NH). ESI MS (MeOH/H_2O, 1:1 v/v): m/z 1151 (MH^+).

Data for $C_{15}H_{31}$CONH-Val-Val-Val-Ala-Ala-Ala-Glu-Glu-Glu-COOH (2). ^{1}H NMR (DMSO-d_6): δ 0.81 (br s, 21H, Val$_\gamma$ + tail CH_3), 1.21 (br s, 31H, C_{14} aliphatic tail), 1.45 (s, 2H, Ala H$_\beta$), 1.75 (m, 6H Glu H$_\beta$), 1.94 (m, 9H, Val$_\beta$ + Glu H$_\beta$), 2.24 (s, 6H, Glu H$_\gamma$), 4.2 (s, 9H, H$_\alpha$), 7.6−8.1 (amide NH). ESI MS (MeOH/H_2O, 1:1 v/v): m/z 1177 (MNa^+).

Data for Asp(CONHC$_{12}$)-Val-Val-Val-Val-Val-Val-Lys-Lys-Lys-NH$_2$ (3). ^{1}H NMR (DMSO-d_6): δ 0.82 (br s, 39H, Val H$_\gamma$ + tail CH_3), 1.22 (br s, 20H, C_{10} aliphatic tail), 1.34 1.53 (m, 6H, Lys H$_\gamma$), 1.69 (m, 6H, Lys H$_\beta$), 1.93 (m, 12H, Lys H$_\delta$ + Val H$_\beta$), 2.74 (m, 2H, tail *CH*$_2$NH), 2.98 (br s, 6H, Lys H$_\epsilon$), 4.09−4.44 (m, 9H, H$_\alpha$), 7.02−8.25 (amide NH). ESI MS (MeOH/H_2O, 1:1 v/v): m/z = 1279 (MH^+).

Data for Asp(CONHC$_{12}$)-Val-Val-Val-Ala-Ala-Ala-Glu-Glu-Glu-NH$_2$ (4). ^{1}H NMR (DMSO-d_6): δ 0.82 (br s, 21H, Val H$_\gamma$ + aliphatic tail CH_3), 1.22 (s, 20H, tail C_{10}), 1.32 (m, 9H, Ala H$_\beta$), 1.74 (m, 3H, Glu H$_\beta$), 1.94 (m, 6H, Glu H$_\beta$ + Val H$_\beta$), 2.25 (m, 6H, Glu H$_\gamma$), 2.97 (d, J = 6 Hz, 2H, tail CH$_2$*CH*$_2$CONH), 4.10−4.44 (m, 9H, H$_\alpha$), 7.23−8.2 (amide NH). ESI MS (MeOH/H_2O, 1:1 v/v): m/z 1197 (MH^+).

Data for Asp(CONHC$_{12}$)-Val-Val-Val-Val-Val-Val-Lys-Lys-Lys-Ser-Gly-Gly-Gly-Tyr-Pro-Val-His-Pro-Ser-Thr (9). ^{1}H NMR (DMSO-d_6): δ 0.82 (br s, 39H, Val H$_\gamma$ + tail CH_3), 1.22 (br s, 20H, C_{10} aliphatic tail), 1.53 (m, 6H, Lys H$_\gamma$), 1.69 (m, 6H, Lys H$_\beta$), 1.93 (m, 16H, Lys H$_\delta$ + Val H$_\beta$ + Pro H$_\gamma$), 2.37 (m, 4H, Pro H$_\beta$), 2.74 (br s, 6H, Lys H$_\epsilon$), 2.98 (m, 2H, tail *CH*$_2$NH), 3.45 (m, 8H, Pro H$_\delta$ + His H$_\beta$ + Tyr H$_\beta$), 3.72 (m, 3H, Thr H$_\alpha$ + Thr H$_\beta$), 4.1−4.6 (m, 13H, H$_\alpha$ + Ser H$_\beta$), 6.81 (m, 5H, Tyr aromatic H's + His H), 7.02−8.25 (amide NH + His H). ESI MS (H_2O): m/z 773.9 $(M + 3H)^{3+}$.

Data for Asp(CONHC$_{12}$)-Val-Val-Val-Ala-Ala-Ala-Lys-Lys-Lys-Ser-Gly-Gly-Gly-Le u-Pro-Leu-Gly-Gln-Ser-His-NH$_2$ (10). ^{1}H NMR (DMSO-d_6): δ 0.82 (br s, 21H, Val H$_\gamma$ + aliphatic tail CH_3), 1.22 (br s, 20H, tail C_{10}), 1.32 (m, 9H, Ala H$_\beta$), 1.53 (m, 6H, Lys H$_\gamma$), 1.64 (m, 6H, Lys H$_\beta$), 1.84 (m, 4H, Leu H$_\beta$), 1.93 (m, 16H, Lys H$_\delta$ + Val H$_\beta$ + Pro H$_\gamma$), 2.37 (m, 2H, Pro H$_\beta$), 2.74 (br s, 6H, Lys H$_\epsilon$), 2.97 (m, 2H, tail CH$_2$*CH*$_2$CONH), 3.45 (m, 4H, Pro H$_\delta$ + His H$_\beta$), 3.72 (m, 3H, His H$_\alpha$ + Ser H$_\beta$), 4.10−4.61 (m, 9H, H$_\alpha$), 6.81 (m, 2H, His H), 7.02−8.25 (amide NH + His H). ESI MS (MeOH/H_2O, 1:1 v/v): m/z 1086.7 $(M + H)^{2+}$.

Circular Dichroism Spectroscopy. Quartz cells with a 0.1 cm path length were used for all experiments. Each spectrum was recorded from 300 to 190 nm at a scan speed of 100 nm/min, a response time of 2 s, and a bandwidth of 1 nm and averaged over five scans. Samples were prepared at a concentration of 0.1 mg/mL in water unless stated otherwise.

Acid−Base Titrations. pK_a titrations were preformed on PAs **1**−**4** in the range of pH 2−10 with a Fisher Accumet pH meter at a concentration of 3.5 mg/mL in 100 mM KCl. For the acidic PAs **2** and **4**, 0.1 N KOH was added in 1−5 μL increments, starting at low pH, whereas for the basic PAs **1** and **3**, 0.1 N HCl was added in 1−5 μL increments, starting at a high pH.

NMR Spectroscopy. PAs **1**−**6** were dissolved in DMSO-d_6 at a concentration of 5 mg/mL. NOESY spectra were measured in D_2O with a mixing time of 0.1 s and 128 scans at a concentration of 10 or 15 mg/mL of each PA, at a 1:1 molar ratio.

IR Spectroscopy. For FT-IR studies, 2 wt % samples were lyophilized from water and then pressed into KBR pellets.

Acknowledgment. This work made use of the Keck Biophysics Facility and the Analytical Services Laboratory at Northwestern University. The work was supported by the U.S. DOE under Award No. DE-FG02-00ER54810.

Supporting Information Available: Additional pH titrations, CD spectra, and FT-IR spectra of peptide amphiphiles (PDF). This material is available free of charge via the Internet at http://pubs.acs.org.

JA044863U